Baryon masses from lattice QCD: Beyond the perturbative chiral regime

Derek B. Leinweber,* Anthony W. Thomas,† Kazuo Tsushima,‡ and Stewart V. Wright§
Department of Physics and Mathematical Physics and Special Research Centre for the Subatomic Structure of Matter, University of Adelaide, Australia 5005

(Received 29 June 1999; revised manuscript received 21 September 1999; published 22 February 2000)

Consideration of the analytic properties of pion-induced baryon self-energies leads to new functional forms for the extrapolation of light baryon masses. These functional forms reproduce the leading non-analytic behavior of chiral perturbation theory, the correct non-analytic behavior at the $N\pi$ threshold and the appropriate heavy-quark limit. They involve only three unknown parameters, which may be obtained by fitting to lattice data. Recent dynamical fermion results from CP-PACS and UKQCD are extrapolated using these new functional forms. We also use these functions to probe the limit of applicability of chiral perturbation theory to the extrapolation of lattice QCD results.

PACS number(s): 12.38.Gc, 11.15.Ha

I. INTRODUCTION

In the last year there has been tremendous progress in the computation of baryon masses within lattice QCD. Improved quark [1] and gluon [2] actions, together with increasing computer speed, means that one already has results for N, Δ and vector meson masses for full QCD with two flavors of dynamical quarks. Although the results are mainly in the regime where the pion mass (m_π) is above 500 MeV, there has been some exploration as low as 300–400 MeV on a 3.0 fm lattice by CP-PACS [3].

In spite of these impressive developments it is still necessary to extrapolate the calculated results to the physical pion mass ($\mu = 140$ MeV) in order to make a comparison with experimental data. In doing so one necessarily encounters some non-linearity in the quark mass (or m_π^2), including the non-analytic behavior associated with dynamical chiral symmetry breaking. Indeed, the recent CP-PACS study [4] did report the first behavior of this kind in baryon systems.

As the computational resources necessary to include three light flavors with realistic masses will not be available for many years, it is vital to develop a sound understanding of how to extrapolate to the physical pion mass. We recently investigated this problem for the case of the nucleon magnetic moments [5].

The cloudy bag model (CBM) [6] is an extension of the MIT bag model incorporating chiral symmetry. It therefore generates the same leading non-analytic (LNA) behavior as chiral perturbation theory (χPT). This model was recently generalized to allow for variable quark and pion masses in order to explore the likely mass dependence of the magnetic moment [5]. This work led to several important results:

(i) A series expansion of $\mu_{p(n)}$ in powers of m_π is not a useful approximation for m_π larger than the physical mass.

(ii) On the other hand, the behavior of the model, after adjustments to fit the lattice data at large m_π, was well determined by the simple Padé approximant

$$\mu_{p(n)} = \frac{\mu_0}{1 + \frac{\alpha}{\mu_0} m_\pi + \beta m_\pi^2}. \tag{1}$$

(iii) Equation (1) not only builds in the Dirac moment at moderately large m_π^2 but has the correct LNA behavior of chiral perturbation theory:

$$\mu = \mu_0 - \alpha m_\pi,$$

with α a model independent constant, as $m_\pi^2 \to 0$.

(iv) Fixing α at the value given by chiral perturbation theory and adjusting μ_0 and β to fit the lattice data yielded values of μ_p and μ_n of $(2.85 \pm 0.22)\mu_N$ and $(-1.96 \pm 0.16)\mu_N$, respectively, at the physical pion mass. These are significantly closer to the experimental values than the usual linear extrapolations in m_q.

Clearly it is vital to extend the lattice calculations of baryon magnetic moments to lower values of m_π than the 600 MeV used in the study just outlined. It is also important to include dynamical quarks. Nevertheless, the apparent success of the extrapolation procedure suggested by the CBM study gives us strong encouragement to investigate the same approach for baryon masses.

Accordingly, in this paper we study the variation of the N and Δ masses with m_π (or equivalently m_q). Section II is devoted to considerations of the low-lying singularities and pion-induced cuts in the complex plane of the nucleon and Δ spectral representation. The analytic properties of the derived phenomenological form are consistent with both chiral perturbation theory and the expected behavior at large m_q. This phenomenological form is eventually fitted to recent two-flavor, full QCD measurements made by CP-PACS [3] and UKQCD [7]. However, to gain some insight into the parameters and behavior of the functional form we examine the N and Δ masses as described in the CBM in Sec. III. In section IV we apply the analytic form to the lattice data. Section V is reserved for a summary of our findings.

*Email address: dleinweb@physics.adelaide.edu.au
†Email address: athomas@physics.adelaide.edu.au
‡Email address: ktsushim@physics.adelaide.edu.au
§Email address: swright@physics.adelaide.edu.au

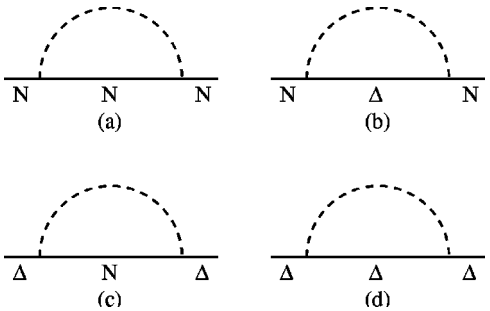

FIG. 1. One-loop pion induced self-energy of the nucleon and the delta.

II. ANALYTICITY

By now it is well established that chiral symmetry is dynamically broken in QCD and that the pion is almost a Goldstone boson. As a result it is strongly coupled to baryons and therefore plays a significant role in the N and Δ self-energies. In the limit where the baryons are heavy, the pion induced self-energies of the N and Δ, to one loop, are given by the processes shown in Fig. 1. Note that we have restricted the intermediate baryon states to those most strongly coupled, namely the N and Δ states.

The analytic expression for the pion cloud correction to the masses of the N and Δ is of the form [8]

$$\delta M_N = \sigma_{NN} + \sigma_{N\Delta}, \tag{2}$$

where

$$\sigma_{NN} = -\frac{3}{16\pi^2 f_\pi^2} g_A^2 \int_0^\infty dk \frac{k^4 u_{NN}^2(k)}{w^2(k)}, \tag{3}$$

$$\sigma_{N\Delta} = -\frac{3}{16\pi^2 f_\pi^2} \frac{32}{25} g_A^2 \int_0^\infty dk \frac{k^4 u_{N\Delta}^2(k)}{w(k)[\Delta M + w(k)]}, \tag{4}$$

and

$$\delta M_\Delta = \sigma_{\Delta\Delta} + \sigma_{\Delta N}, \tag{5}$$

where

$$\sigma_{\Delta\Delta} = \sigma_{NN}, \tag{6}$$

$$\sigma_{\Delta N} = \frac{3}{16\pi^2 f_\pi^2} \frac{8}{25} g_A^2 \int_0^\infty dk \frac{k^4 u_{N\Delta}^2(k)}{w(k)[\Delta M - w(k)]}. \tag{7}$$

We note that $\Delta M = M_\Delta - M_N$, $g_A = 1.26$ is the axial charge of the nucleon, $w(k) = \sqrt{k^2 + m_\pi^2}$ is the pion energy and $u_{NN}(k)$, $u_{N\Delta}(k)$, ... are the $NN\pi$, $N\Delta\pi$, ... form factors associated with the emission of a pion of three-momentum k. We have used SU(6) symmetry to relate the four coupling constants to the $NN\pi$ coupling, which, in turn, has been related to $g_A/2f_\pi$ by chiral symmetry. The form factors arise naturally in any chiral quark model because of the finite size of the baryonic source of the pion field—which suppresses the emission probability at high virtual pion momentum. As a result, the self-energy integrals are not divergent.

The leading non-analytic contribution (LNAC) of these self-energy diagrams is associated with the infrared behavior of the corresponding integrals—i.e., the behavior as $k \to 0$. As a consequence, the leading non-analytic behavior should not depend on the details of the high momentum cutoff or the form factors. In particular, it should be sufficient for studying the LNAC to evaluate the self-energy integrals using a simple sharp cutoff, $u(k) = \theta(\Lambda - k)$. In Sec. III we shall compare the results with those calculated using a phenomenological, dipole form factor and show that this is in fact an effective simplification.

Using a θ function for the form factors, the $NN\pi$ and $\Delta\Delta\pi$ integrals [cf. Figs. 1(a) and 1(d), respectively], which are equal, are easily evaluated in the heavy baryon approximation used here:

$$\sigma_{NN} = \sigma_{\Delta\Delta} = -\frac{3}{16\pi^2 f_\pi^2} g_A^2 \int_0^\Lambda dk \frac{k^4}{w^2(k)} = -\frac{3g_A^2}{16\pi^2 f_\pi^2}\left[m_\pi^3 \arctan\left(\frac{\Lambda}{m_\pi}\right) + \frac{\Lambda^3}{3} - \Lambda m_\pi^2 \right]. \tag{8}$$

The integral corresponding to the process shown in Fig. 1(b), with a θ function form factor, may be analytically evaluated. For $m_\pi > \Delta M$,

$$\sigma_{N\Delta} = -\frac{g_A^2}{25\pi^2 f_\pi^2}\left\{ 12(m_\pi^2 - \Delta M^2)^{3/2}\left[\arctan\left(\frac{\sqrt{m_\pi^2 + \Lambda^2} + \Delta M + \Lambda}{\sqrt{m_\pi^2 - \Delta M^2}} \right) - \arctan\left(\frac{\Delta M + m_\pi}{\sqrt{m_\pi^2 - \Delta M^2}} \right) \right] + 3\Delta M(3m_\pi^2 - 2\Delta M^2) \ln\left(\frac{\sqrt{m_\pi^2 + \Lambda^2} + \Lambda}{m_\pi} \right) - 3\sqrt{m_\pi^2 + \Lambda^2}\,\Delta M \Lambda + 6\Delta M^2 \Lambda - 6m_\pi^2 \Lambda + 2\Lambda^3 \right\}, \tag{9}$$

while for $m_\pi < \Delta M$ we find

$$\sigma_{N\Delta}=-\frac{g_A^2}{25\pi^2 f_\pi^2}\left\{-6(\Delta M^2-m_\pi^2)^{3/2}\left[\ln\left(\frac{\sqrt{\Delta M^2-m_\pi^2}+\sqrt{m_\pi^2+\Lambda^2}+\Delta M+\Lambda}{\sqrt{\Delta M^2-m_\pi^2}-\sqrt{m_\pi^2+\Lambda^2}-\Delta M-\Lambda}\right)-\ln\left(\frac{\sqrt{\Delta M^2-m_\pi^2}+\Delta M+m_\pi}{\sqrt{\Delta M^2-m_\pi^2}-\Delta M-m_\pi}\right)\right]\right.$$
$$\left.+3\Delta M(3m_\pi^2-2\Delta M^2)\ln\left(\frac{\sqrt{m_\pi^2+\Lambda^2}+\Lambda}{m_\pi}\right)-3\sqrt{m_\pi^2+\Lambda^2}\Delta M\Lambda+6\Delta M^2\Lambda-6m_\pi^2\Lambda+2\Lambda^3\right\}. \quad (10)$$

Similar results are easily obtained for the process shown in Fig. 1(c). For $m_\pi>\Delta M$, the analytic form is

$$\sigma_{\Delta N}=\frac{g_A^2}{100\pi^2 f_\pi^2}\left\{-12(m_\pi^2-\Delta M^2)^{3/2}\left[\arctan\left(\frac{\sqrt{m_\pi^2+\Lambda^2}-\Delta M+\Lambda}{\sqrt{m_\pi^2-\Delta M^2}}\right)+\arctan\left(\frac{\Delta M-m_\pi}{\sqrt{m_\pi^2-\Delta M^2}}\right)\right]\right.$$
$$\left.+3\Delta M(3m_\pi^2-2\Delta M^2)\ln\left(\frac{\sqrt{m_\pi^2+\Lambda^2}+\Lambda}{m_\pi}\right)-3\sqrt{m_\pi^2+\Lambda^2}\Delta M\Lambda-6\Delta M^2\Lambda+6m_\pi^2\Lambda-2\Lambda^3\right\}, \quad (11)$$

while for $m_\pi<\Delta M$

$$\sigma_{\Delta N}=\frac{g_A^2}{100\pi^2 f_\pi^2}\left\{6(\Delta M^2-m_\pi^2)^{3/2}\left[\ln\left(\frac{\sqrt{\Delta M^2-m_\pi^2}+\sqrt{m_\pi^2+\Lambda^2}-\Delta M+\Lambda}{\sqrt{\Delta M^2-m_\pi^2}-\sqrt{m_\pi^2+\Lambda^2}+\Delta M-\Lambda}\right)+\ln\left(\frac{\sqrt{\Delta M^2-m_\pi^2}+\Delta M-m_\pi}{\sqrt{\Delta M^2-m_\pi^2}-\Delta M+m_\pi}\right)\right]\right.$$
$$\left.+3\Delta M(3m_\pi^2-2\Delta M^2)\ln\left(\frac{\sqrt{m_\pi^2+\Lambda^2}+\Lambda}{m_\pi}\right)-3\sqrt{m_\pi^2+\Lambda^2}\Delta M\Lambda-6\Delta M^2\Lambda+6m_\pi^2\Lambda-2\Lambda^3\right\}. \quad (12)$$

The self-energies involving transitions of $N\to\Delta$ or $\Delta\to N$ are characterized by the branch point at $m_\pi=\Delta M$.

A. Chiral limit

Chiral perturbation theory is concerned with the behavior of quantities such as the baryon self-energies as $m_q\to 0$. For the expressions derived above, this corresponds to taking the limit $m_\pi\to 0$. The leading non-analytic terms are those which correspond to the lowest order non-analytic functions of m_q—i.e., odd powers or logarithms of m_π. By expanding the expressions given above, we find that the LNA contribution to the nucleon/Δ mass [Eq. (8)] is given by

$$M_{N(\Delta)}^{LNA}=-\frac{3}{32\pi f_\pi^2}g_A^2 m_\pi^3, \quad (13)$$

in agreement with a well-known result of χPT [9]. A careful expansion of the $\Delta\pi$ contribution to the nucleon self-energy, Eq. (9), yields the LNA term

$$\sigma_{N\Delta}(m_\pi,\Lambda)\sim\frac{3g_A^2}{16\pi^2 f_\pi^2}\frac{32}{25}\frac{3}{8\Delta M}m_\pi^4\ln(m_\pi) \quad (14)$$

as $m_\pi\to 0$ which is again as expected from χPT [10]. For the $N\pi$ contribution to the self-energy of the Δ, the LNA term in the chiral limit of Eq. (11) yields

$$\sigma_{\Delta N}(m_\pi,\Lambda)\sim-\frac{3g_A^2}{16\pi^2 f_\pi^2}\frac{8}{25}\frac{3}{8\Delta M}m_\pi^4\ln(m_\pi). \quad (15)$$

Of course, our concern with respect to lattice QCD is not so much the behavior as $m_\pi\to 0$, but the extrapolation from high pion masses to the physical pion mass. In this context the branch point at $m_\pi^2=\Delta M^2$ is at least as important as the LNA near $m_\pi=0$. We shall return to this point later. We note that Banerjee and Milana [11] found the same non-analytic behavior as $m_\pi\to\Delta M$ that we find. However, they were not concerned with finding a form that could be used at large pion masses—i.e. one that is consistent with heavy quark effective theory.

B. Heavy quark limit

Heavy quark effective theory suggests that as $m_\pi\to\infty$ the quarks become static and hadron masses become proportional to the quark mass. This has been rather well explored in the context of successful nonrelativistic quark models of charmonium and bottomium [12]. In this spirit, corrections are expected to be of order $1/m_q$ where m_q is the heavy quark mass. Thus we would expect the pion induced self-energy to vanish as $1/m_q$ as the pion mass increases. The presence of a fixed cutoff Λ acts to suppress the pion induced self-energy for increasing pion masses, as evidenced by the m_π^2 in the denominators of Eqs. (3), (4) and (7). While some m_π^2 dependence in Λ is expected, this is a second-order effect and does not alter the qualitative features. By expanding the $\arctan(\Lambda/m_\pi)$ term in Eq. (8) for small Λ/m_π, we find

$$\sigma_{NN}=-\frac{3g_A^2}{16\pi^2 f_\pi^2}\frac{\Lambda^5}{5m_\pi^2}+\mathcal{O}\left(\frac{\Lambda^7}{m_\pi^4}\right), \quad (16)$$

which vanishes for $m_\pi \to \infty$. Indeed, in the large m_π (heavy quark) limit, both Eqs. (9) and (11) tend to zero as $1/m_\pi^2$.

C. Analytic form

We now have the chiral and heavy quark limits for each of the four integrals in Fig. 1. These expressions, which contain a single parameter, Λ, are correct in the chiral limit—i.e., they reproduce the first two non-analytic terms of χPT. They also have the correct behavior in the limit of large pion mass; namely they vanish like $1/m_\pi^2$. The latter feature would be destroyed if we were to retain only the LNA pieces of the self-energies as they would diverge at large m_π faster than m_q. Rather than simplifying our expressions to just the LNA terms, we therefore retain the complete expressions, as they contain important physics that would be lost by making a simplification.

We note that keeping the entire form is not in contradiction with χPT, as we have already shown that the leading non-analytic structure of χPT is contained in this form. However, as one proceeds to larger quark (pion) masses, differences between the full forms and the expressions in the chiral limit will become apparent. For example, the branch point at $m_\pi^2 = \Delta M^2$, which is an essential non-analytic component of the m_π dependence of the self-energy and which should dominate in the region $m_\pi \sim \Delta M$, is also satisfactorily incorporated in Eqs. (9) and (11). Yet the LNA chiral terms given in Sec. II A know nothing of this branch point and are clearly inappropriate in the region near and beyond $m_\pi^2 = \Delta M^2$.

As a result of these considerations, we propose to use the analytic expressions for the self-energy integrals corresponding to a sharp cutoff in order to incorporate the correct LNA structure in a simple three-parameter description of the m_π dependence of the N and Δ masses. In the heavy quark limit hadron masses become proportional to the quark mass. Moreover, as we shall see in the next section, the MIT bag model leads to a linear dependence of the mass of a baryon on the current quark mass far below the scale at which one would expect the heavy quark limit to apply. This is a simple consequence of relativistic quantum mechanics for a scalar confining field. On the other hand, lattice calculations indicate that the scale at which the pion mass exhibits a linear dependence on m_q is much larger than that for baryons.[1] In fact, over the range of masses of interest to us, explicit lattice calculations show that m_π^2 is proportional to m_q. Hence we can simulate a linear dependence of the baryon masses on the quark mass, m_q, in this region, by adding a term involving m_π^2. The functional form for the mass of the nucleon suggested by this analysis is then

$$M_N = \alpha_N + \beta_N m_\pi^2 + \sigma_{NN}(m_\pi,\Lambda) + \sigma_{N\Delta}(m_\pi,\Lambda), \quad (17)$$

while that for the Δ is

$$M_\Delta = \alpha_\Delta + \beta_\Delta m_\pi^2 + \sigma_{\Delta\Delta}(m_\pi,\Lambda) + \sigma_{\Delta N}(m_\pi,\Lambda). \quad (18)$$

The mass in the chiral limit is given by

$$M_N^{(0)} = \alpha_N + \sigma_{NN}(0,\Lambda) + \sigma_{N\Delta}(0,\Lambda), \quad (19)$$

where the meson cloud effects are explicitly contained in $\sigma_{NN}(0,\Lambda) + \sigma_{N\Delta}(0,\Lambda)$. The mass of the Δ in the chiral limit is calculated in an analogous way. We know that Eqs. (17) and (18) have the correct behavior in the chiral limit. Individually, they also have the correct heavy quark behavior.[2] Between the chiral and heavy-quark limits there are no general guidelines, so in the next section we shall compare our functional form to the cloudy bag model, a successful phenomenological approach incorporating chiral symmetry and the correct heavy quark limit.

III. BARYON MASSES WITHIN THE CBM

As a guide to the quark mass dependence of the N and Δ masses we consider the cloudy bag model [6,13]. This is a minimal extension of the MIT bag model such that chiral symmetry is restored, which has proved quite successful in a number of phenomenological studies of baryon properties and meson-baryon scattering [6,15–17]. Within the CBM, a baryon is viewed as a superposition of a bare quark core and bag plus meson states. The linearized CBM Lagrangian with pseudovector pion-quark coupling (to order $1/f_\pi$) is [18]

$$\begin{aligned}\mathcal{L} = {} & [\bar{q}(i\gamma^\mu \partial_\mu - m_q)q - B]\theta_V \\ & - \frac{1}{2}\bar{q}q\,\delta_S + \frac{1}{2}(\partial_\mu \boldsymbol{\pi})^2 - \frac{1}{2}m_\pi^2 \boldsymbol{\pi}^2 \\ & + \frac{\theta_V}{2f_\pi}\bar{q}\gamma^\mu \gamma_5 \boldsymbol{\tau} q \cdot \partial_\mu \boldsymbol{\pi}, \end{aligned} \quad (20)$$

where B is the bag constant, f_π is the π decay constant, θ_V is a step function (unity inside the bag volume and vanishing outside) and δ_S is a surface delta function. In a lowest order perturbative treatment of the pion field, the quark wave function is not effected by the pion field and is simply given by the MIT bag solution [19–21].

In principle the πNN form factor can be directly calculated within the model. It dies off at large momentum transfer because of the finite size of the baryon source. Rather

[1] One does not expect such linear behavior to appear for quark masses lighter than the charm quark mass where the pseudoscalar mass is 3.0 GeV. Even at this scale the quarks are still somewhat relativistic.

[2] With regard to the difference, $M_\Delta - M_N$, heavy quark effective theory (HQET) suggests that this difference should vanish as $m_\pi \to \infty$. This is only guaranteed by Eqs. (17) and (18) [through Eq. (16)] if the entire mass difference arises from the pion self-energy. While one could enforce this condition through the introduction of additional parameters and a more complicated analytic structure for the higher-order terms of Eqs. (17) and (18), we prefer to focus on the regime of m_π^2 from 1 GeV^2 to the chiral limit. As we shall see, Eqs. (17) and (18) are quite adequate for this purpose.

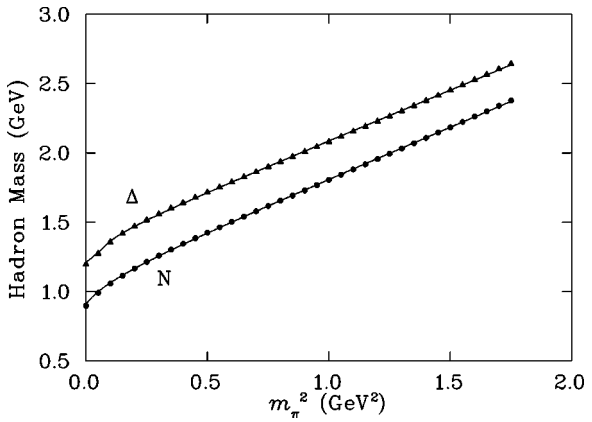

FIG. 2. The pion mass dependence of the N and Δ baryons generated in the CBM using a dipole form factor with $\Lambda_D = 1$ GeV. Fits of Eqs. (17) and (18) to the CBM results are illustrated by the curves.

than using this calculated form factor, which is model dependent, we have chosen to use a common phenomenological form, namely a simple dipole

$$u(k) = \frac{(\Lambda_D^2 - \mu^2)^2}{(\Lambda_D^2 + k^2)^2}, \tag{21}$$

where k is the magnitude of the loop (3-)momentum, μ is the physical pion mass (139.6 MeV), and Λ_D is a regulation parameter.

In the standard CBM treatment, where the pion is treated as an elementary field, the current quark mass, m_q, is not directly linked to m_π. Most observables are not sensitive to this parameter, as long as it is in the range of typical current quark masses. For our present purpose it is vital to relate the m_q inside the bag with m_π. Current lattice simulations indicate that m_π^2 is approximately proportional to m_q over a wide range of quark masses [3]. Hence, in order to model the lattice results, we scale the mass of the quark confined in the bag as $m_q = (m_\pi/\mu)^2 m_q^{(0)}$, with $m_q^{(0)}$ being the current quark mass corresponding to the physical pion mass μ. $m_q^{(0)}$ is treated as an input parameter to be tuned to the lattice results, but in our magnetic moment study it turned out to lie in the range 6–7 MeV, which is very reasonable.

The parameters of the CBM are obtained as follows. The bag constant B and the phenomenological parameter z_0 are fixed by the physical nucleon mass and the stability condition,[3] $dM_N/dR = 0$, for a given choice of R_0 and $m_q^{(0)}$. For each subsequent value of the pion mass or the quark mass considered, ω_0 and R are determined simultaneously from the linear boundary condition [19–21] and the stability condition. In this work we have calculated the mass of the N and Δ baryons as a function of squared pion mass (as illustrated in Fig. 2). The Δ calculation is similar to that for the N; however, the value of B is fixed to be the same as that used for the nucleon, while z_0 is adjusted to fit the observed mass difference, taking into account the pionic contribution to this quantity, at the physical value $m_\pi = \mu$ $(m_q = m_q^{(0)})$.

TABLE I. Parameters for fitting Eqs. (17) and (18) to the CBM data. Here we have taken $R_0 = 1.0$ fm and $m_q^{(0)} = 6.0$ MeV. The Error column denotes the relative difference from the experimental values which were used as a constraint in generating the CBM data.

Baryon	α (GeV)	β (GeV^{-1})	Λ (GeV)	M_B (GeV)	Error
N	1.09	0.739	0.455	0.948	0.8%
Δ	1.37	0.725	0.419	1.236	0.3%

As expected on quite general grounds (and discussed in Sec. II), as the pion mass increases the mass of the baryon does indeed become linear in m_π^2. In addition, from the curvature at low pion mass, we see that the non-analytic structure is important in the region m_π below 400 MeV.

We now fit our functional forms for the baryon masses, Eqs. (17) and (18), to the CBM data. We note that the CBM data are generated using a phenomenologically motivated, dipole form factor, whereas the functional form used in the fit involves a θ cutoff. In order to simulate the fitting procedure for lattice data, our fit to the CBM results involves only pion masses above the physical branch point at $M_\Delta = M_N$, followed by an extrapolation to lower pion mass.

It can be seen from Fig. 2 that our extrapolation to the physical pion mass is in good agreement with the CBM calculations: at the physical pion mass the extrapolated N mass is within 0.8% of the experimental value to which the CBM was fitted, while the Δ is within 0.3% of the experimental value. We present the parameters of our fit in Table I. The value for the sharp cutoff (Λ) is 0.44(2) GeV, compared to $\Lambda_D = 1$ GeV for the dipole form factor.

It was noted in Sec. II that the constant α in our functional form is not the mass of the baryon in the chiral limit, but rather this is given by $M_N^{(0)} = \alpha_N + \sigma_{NN}(0,\Lambda)$

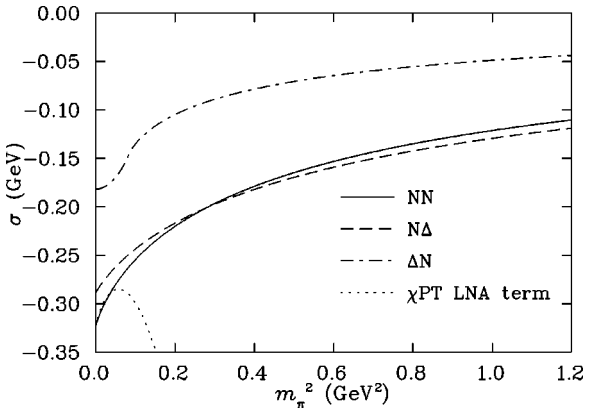

FIG. 3. Pion induced self-energy corrections for a 1 GeV dipole form factor. The LNA term of χPT tracks the $NN\pi$ contribution up to $m_\pi \sim 0.2$ GeV, beyond which the internal structure of the nucleon becomes important.

[3]Note that while z_0, B and the πNN form factor may all depend on m_q, this dependence is expected to be a smaller effect and we ignore such variations in order to avoid an excess of parameters.

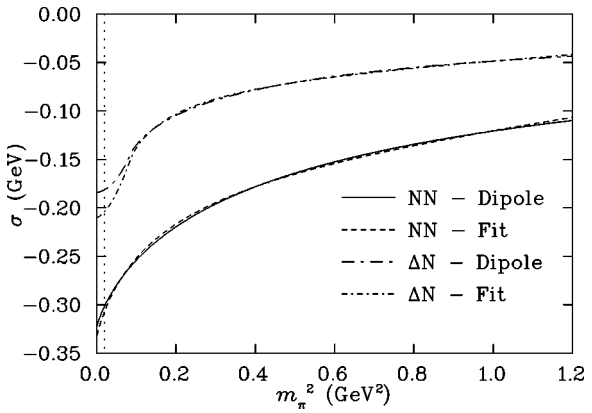

FIG. 4. Comparison between the nucleon and Δ self-energies, σ_{NN} and $\sigma_{\Delta N}$, calculated using a dipole form factor (solid and long-dash-dotted curves, respectively) and fits using the form $\alpha+\beta m_\pi^2+\sigma_{ij}(m_\pi,\Lambda)$, based on a sharp cut-off in the momentum of the virtual pion (dashed and short-dash-dotted curves respectively).

$+\sigma_{N\Delta}(0,\Lambda)$—with an analogous expression for the Δ. We find that the extrapolated N and Δ masses in the chiral [SU(2)-flavor] limit are $(M_N^{(0)},M_\Delta^{(0)})=(905,1210)$ MeV, compared with the CBM values (898,1197) MeV.

The mass dependence of the pion induced self-energies, σ_{ij}, for the 1 GeV dipole form factor, is displayed in Fig. 3. The choice of a 1 GeV dipole corresponds to the observed axial form factor of the nucleon [22], which is probably our best phenomenological guide to the pion-nucleon form factor [23]. We note that σ_{NN} tends to zero smoothly as m_π grows and it is only below $m_\pi^2\sim 0.3$ GeV^2 that there is any rapid variation. That this behavior cannot be well described by a polynomial expansion is illustrated by the dotted curve in Fig. 3. There we expanded σ_{NN} about $m_\pi=0$ as a simple polynomial, $\alpha+\beta m_\pi^2+\gamma m_\pi^3$, with γ fixed at the value required by chiral symmetry. Clearly the expansion fails badly for m_π beyond 300–400 MeV.

The behavior of the $N\pi$ contribution to the self-energy of the Δ is especially interesting. In particular, the effect of the branch point at $m_\pi=\Delta M$ is seen in the curvature at $m_\pi^2\sim 0.1$ GeV^2. For comparison, we note that while there is also a branch point in the nucleon self-energy at the same point—see Eq. (9)—the coefficient of $(m_\pi^2-\Delta M^2)^{3/2}$ vanishes at this point. As a consequence there is little or no curvature visible in the latter quantity at the same point. The correct description of this curvature is clearly very important if one wishes to obtain the ΔN mass difference at the physical pion mass. The fact that, as shown in Fig. 2, our simple three parameter phenomenological fitting function can reproduce N and Δ masses within the CBM, including this curvature, suggests that this should also provide a reliable form for extrapolating lattice data into the region of small pion mass.

Figure 4 illustrates the degree of residual model dependence in our use of Eqs. (17) and (18). There the variation of the nucleon self-energy, σ_{NN}, calculated with a 1 GeV dipole form factor (solid curve) is fit using the form $\alpha+\beta m_\pi^2+\sigma_{NN}(m_\pi,\Lambda)$ (dashed curve, with $\alpha=-0.12$ GeV, $\beta=0.39$ GeV^{-1} and $\Lambda=0.57$ GeV). Note that the devia-

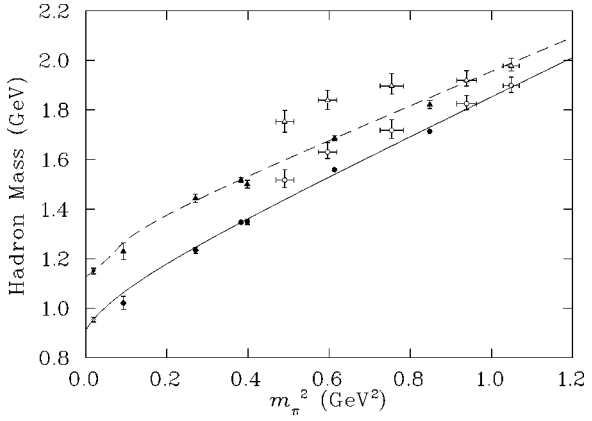

FIG. 5. Baryon masses calculated by UKQCD (open points) and CP-PACS (solid points), as a function of m_π^2. The solid (dashed) curve illustrates a fit to the combined data sets for N (Δ). The leftmost data points are our extrapolated values of the baryon masses at the physical pion mass.

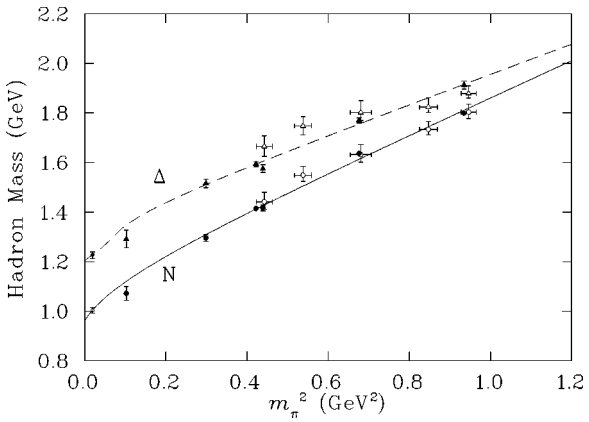

FIG. 6. UKQCD and CP-PACS baryon masses with 5% adjustments in the scale parameters to improve the agreement between the two data sets. (The key is as described in Fig. 5.)

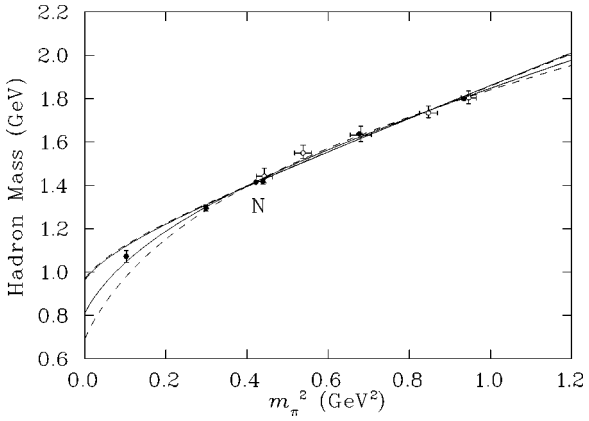

FIG. 7. UKQCD and CP-PACS nucleon masses with scale parameters adjusted by 5%. The data are as described in Fig. 5. The dashed lines represent fits without the point at 0.1 GeV^2. The solid lines include this point. The top pair of lines are fits with Λ fixed at 0.455 GeV, a value preferred on the basis of our CBM analysis. The bottom pair have Λ as a fit parameter.

TABLE II. Parameters for fits of Eqs. (17) and (18) to lattice data. Here we fix Λ ($\Lambda_N=0.455$ and $\Lambda_\Delta=0.419$) and vary α and β. The mass of the baryon at the physical pion mass is M_N (M_Δ) and the mass in the chiral limit is $M_N^{(0)}$ ($M_\Delta^{(0)}$). The scaling columns represent adjustments to the scale parameters providing physical dimensions to the lattice data.

Scaling		N				Δ			
CP-PACS	UKQCD	α (GeV)	β (GeV^{-1})	M_N (GeV)	$M_N^{(0)}$ (GeV)	α (GeV)	β (GeV^{-1})	M_Δ (GeV)	$M_\Delta^{(0)}$ (GeV)
0%	0%	1.10	0.778	0.954	0.910	1.29	0.680	1.150	1.125
+5%	−5%	1.15	0.736	1.003	0.961	1.36	0.602	1.227	1.203
0%	−10%	1.10	0.767	0.957	0.914	1.31	0.624	1.169	1.145
+10%	0%	1.20	0.707	1.050	1.008	1.42	0.581	1.285	1.262

tions are at the level of a few MeV. For the Δ the self-energy, $\sigma_{\Delta N}$, is again calculated using a 1 GeV dipole form factor and fit with our standard fitting function, $\alpha+\beta m_\pi^2+\sigma_{\Delta N}(m_\pi,\Lambda)$. The quality of the fit (with $\alpha=-0.062$ GeV, $\beta=0.024$ GeV^{-1} and $\Lambda=0.53$ GeV) is not as good as for the nucleon case. Nevertheless, the difference between the two curves at the physical pion mass (vertical dotted line) is only about 20 MeV. At the present stage of lattice calculations this seems to be an acceptable level of form factor dependence for such a subtle extrapolation.

IV. LATTICE DATA ANALYSIS

We consider two independent lattice simulations of the N and Δ masses, both of which use improved actions to study baryon masses in full QCD with two light flavors. The CP-PACS [3] lattice data are generated on a plaquette plus rectangle gauge action with improvement coefficients based on an approximate block-spin renormalization group analysis. The $\mathcal{O}(a)$-improved Sheikholeslami-Wohlert clover action is used with a mean-field improved estimate of the clover coefficient $c_{SW}=1.64$–1.69. This estimate is likely to lie low relative to a nonperturbative determination [14] and may leave residual $\mathcal{O}(a)$ errors.

Ideally one would like to work with lattice data in which the infinite-volume continuum limit is taken prior to the chiral limit. Until such data are available, we select results from their $12^3\times32$ and $16^3\times32$ simulations at $\beta=1.9$. Lattice spacings range from 0.25 fm to 0.19 fm and provide physical volumes of 2.7 fm to 3.5 fm on a side. While the volumes are large enough to avoid significant finite volume errors, the coarse lattice spacings necessitate the use of improved actions. Systematic uncertainties the order of 10% are not unexpected.

The UKQCD [7] group uses a standard plaquette action with the $\mathcal{O}(a)$-improved Sheikholeslami-Wohlert action. At a β of 5.2, UKQCD uses $c_{SW}=1.76$, which is lower than the current non-perturbative value [14] of 2.017, again leaving some residual $\mathcal{O}(a)$ errors. Lattice spacings are necessarily smaller, ranging from 0.13 to 0.21 fm. We select their $12^3\times24$ data set as providing better statistical errors than their largest volume simulation. Physical volumes are 1.6–2.6 fm on a side, suggesting that finite volume errors may be an issue on the smallest physical volume where the dynamical quark mass is lightest.

In full QCD, the renormalized lattice spacing is a function of both the bare coupling and the bare quark mass. In order to determine the lattice spacing, the UKQCD Collaboration

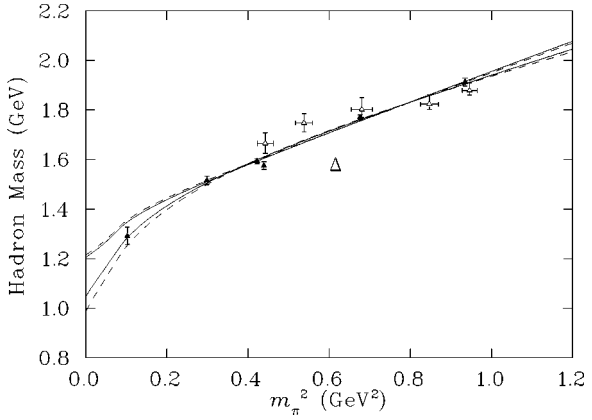

FIG. 8. UKQCD and CP-PACS Δ-baryon masses with scale parameters adjusted by 5%. The data are as described in Fig. 5. The dashed lines represent fits without the point at 0.1 GeV^2. The solid lines include this point. The top pair of lines are fits with Λ fixed at 0.419 GeV, a value preferred on the basis of our CBM analysis. The bottom pair have Λ as a fit parameter.

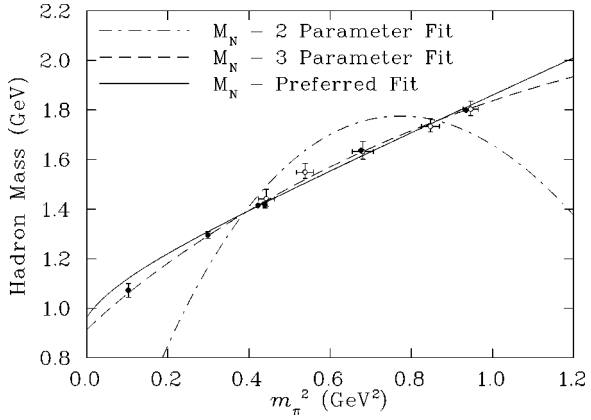

FIG. 9. A comparison between phenomenological fitting functions for the mass of the nucleon. The two parameter fit corresponds to using Eq. (22) with γ set equal to the value known from χPT. The three parameter fit corresponds to letting γ vary as an unconstrained fit parameter. The solid line is the fit for the functional form of Eq. (17), fit (d) of Table III.

TABLE III. Parameters for the fits shown in Fig. 7. Parameter sets (a) and (b) are obtained by excluding the lowest data point from the fit, while (c) and (d) include it. Parameter sets (a) and (c) are fits with 3 parameters, and sets (b) and (d) are fits with Λ fixed to the phenomenologically preferred value.

Fit	α (GeV)	β (GeV^{-1})	Λ (GeV)	M_N (GeV)
(a)	1.76	0.386	0.789	0.763
(b)	1.15	0.727	0.455	1.010
(c)	1.42	0.564	0.661	0.870
(d)	1.15	0.736	0.455	1.003

TABLE IV. Parameters for the fits shown in Fig. 8. Parameter sets (a) and (b) are obtained by excluding the lowest data point from the fit, while (c) and (d) include it. Parameter sets (a) and (c) are fits with 3 parameters, and sets (b) and (d) are fits with Λ fixed to the phenomenologically preferred value.

Fit	α (GeV)	β (GeV^{-1})	Λ (GeV)	M_Δ (GeV)
(a)	1.64	0.414	0.683	1.042
(b)	1.37	0.587	0.419	1.240
(c)	1.54	0.475	0.616	1.095
(d)	1.36	0.602	0.419	1.230

calculates the force between two static quarks at a distance r_0 [24], while CP-PACS considers the string tension directly. While the two approaches yield similar results in the quenched approximation, string breaking in full QCD may introduce some systematic error in the extraction of the string tension at large distances. In fact we find that the two data sets are consistent, provided one allows the parameters introducing the physical scale to float within systematic errors of 10%. A thorough investigation of these systematic errors lies outside the scope of this investigation. Instead we simply rescale the UKQCD and CP-PACS data sets in combining them into a single, consistent data set.

We begin by considering the functional form suggested in Sec. II with the cutoff Λ fixed to the value determined by fitting the CBM calculations. The resulting fits to the baryon masses are shown in Fig. 5 for the unshifted lattice data and Fig. 6 where each data set is adjusted by 5% to provide consistency. The extrapolations are indicated by the solid (dashed) curve for N (Δ). The resulting fit parameters and masses[4] are listed in Table II.

In examining fits in which the cutoff is allowed to vary as a fit parameter, we found it instructive to also study the dependence of the fit on the number of points included. This dependence is shown for the N in Fig. 7 and for the Δ in Fig. 8. In particular, we compare fits including the lowest lattice point (at around 0.1 GeV^2) and then excluding it. When we fix the value of Λ the fits are stable and insensitive to the lowest point. They tend to lie slightly above the lowest data point. However, given the caution expressed by the CP-PACS Collaboration for the lowest point, we view these fits as reasonably successful. In contrast, when the value of Λ is treated as a fitting parameter, it is sensitive to the inclusion of the lowest point. Hence, to perform model independent fits, it is essential to have lattice simulations at light quark masses approaching $m_\pi^2 \sim 0.1$ GeV^2. An analysis of the current data suggests $\Lambda = 0.661$ GeV and provides a nucleon mass 130 MeV lower than the CBM-constrained fit. Tables III and IV summarize parameters and physical baryon masses for N and Δ respectively.

[4]The errors bars for the extrapolated baryon masses at the physical pion mass displayed in the figures are naive estimates only. We are unable to perform a complete analysis without the lattice results on a configuration by configuration basis.

It is common practice in the lattice community to use a polynomial expansion for the mass dependence of hadron masses. Motivated by χPT the lowest odd power of m_π allowed is m_π^3:

$$M_N = \alpha + \beta m_\pi^2 + \gamma m_\pi^3 . \tag{22}$$

The results of such fits are shown in Figs. 9 and 10 for N and Δ respectively. The corresponding parameters are reported in Table V. As can be seen in Table V, the coefficient of the m_π^3 term, which is the leading non-analytic term in the quark mass, disagrees with the coefficient known from χPT by almost an order of magnitude. This clearly indicates the failings of such a simple fitting procedure. We recommend that future fitting and extrapolation procedures should be based on Eqs. (17) and (18), which are consistent with χPT and the heavy quark limit.

V. SUMMARY

In the quest to connect lattice measurements with the physical regime, we have explored the quark mass dependence of the N and Δ baryon masses using arguments based on analyticity and heavy quark limits. In the region where

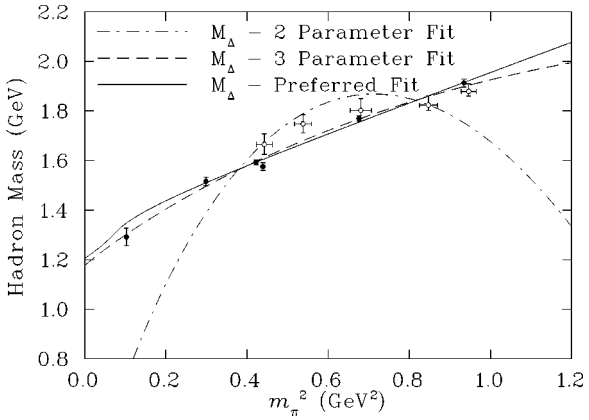

FIG. 10. A comparison between phenomenological fitting functions for the mass of the Δ. The two parameter fit corresponds to using Eq. (22) with γ set equal to the value known from χPT. The three parameter fit corresponds to letting γ vary as an unconstrained fit parameter. The solid line is the fit for the functional form of Eq. (18), fit (d) of Table IV.

TABLE V. Parameter sets for the fits shown in Figs. 9 and 10. Set (a) is for the 2 parameter fit of Eq. (22) with γ from χPT, (b) for the 3 parameter fit of Eq. (22), and (c) for the preferred functional form.

	N				Δ			
Fit	α (GeV)	β (GeV^{-1})	γ or Λ (GeV^{-2}) or (GeV)	M_N (GeV)	α (GeV)	β (GeV^{-1})	γ or Λ (GeV^{-2}) or (GeV)	M_Δ (GeV)
(a)	-0.128	7.38	-5.60	-0.001	0.182	7.09	-5.60	0.304
(b)	0.912	1.69	-0.761	0.943	1.18	1.45	-0.703	1.202
(c)	1.15	0.736	0.455	1.003	1.37	0.602	0.419	1.227

m_π is larger than 500 MeV, the lattice data can be reasonably well described by the simple form $\alpha+\beta m_\pi^2$, which is linear in the quark mass. The additional curvature associated with chiral corrections only appears below this region. This can be understood quite naturally within chiral quark models, like the cloudy bag, which lead to a cutoff on high momentum virtual pions, thus suppressing the self-energy diagrams quite effectively as m_π^2 increases. The pionic self-energy diagrams which we consider are unique in that only these diagrams give rise to the leading non-analytic behavior which yields a rapid variation of baryon masses in the chiral limit. Loops involving heavier mesons or baryons cannot give rise to such a rapid variation.

Based on these considerations, we have determined a method to access quark masses beyond the regime of chiral perturbation theory. This method reproduces the leading non-analytic behavior of χPT and accounts for the internal structure of the baryon under investigation. We find that the predictions of the CBM, and two flavor, dynamical fermion lattice QCD results, are succinctly described by the formulas of Eqs. (17) and (18) with terms defined in Eqs. (8)–(12). We believe that Eqs. (8)–(12) are the simplest one can write down which involve a single parameter, yet incorporate the essential constraints of chiral symmetry and the heavy quark limit.

Firm conclusions concerning agreement between the extrapolated lattice results and experiment cannot be made until the systematic errors can be reduced below the current level of 10% and accurate measurements are made at $m_\pi \sim 300$ MeV or lower. The significance of non-linear behavior in extrapolating nucleon and Δ masses as a function of m_π^2 to the chiral regime has been evaluated. We find that the leading non-analytic term of the chiral expansion dominates from the chiral limit up to the branch point at $m_\pi=\Delta M$. The curvature around $m_\pi=\Delta M$, neglected in previous extrapolations of the lattice data, leads to shifts in the extrapolated masses of the same order as the departure of lattice estimates from experimental measurements.

ACKNOWLEDGMENTS

We would like to thank Pierre Guichon and Tom Cohen for helpful discussions. This work was supported in part by the Australian Research Council.

[1] B. Sheikholeslami and R. Wohlert, Nucl. Phys. **B259**, 609 (1985).
[2] M. Alford, W. Dimm, and P. Lepage, Phys. Lett. B **361**, 87 (1995); P. Hasenfratz, Nucl. Phys. B (Proc. Suppl.) **63**, 53 (1998).
[3] CP-PACS Collaboration, S. Aoki *et al.* Phys. Rev. D **60**, 114508 (1999).
[4] CP-PACS Collaboration, Yoshinobu Kuramashi for the collaboration, hep-lat/9904003.
[5] D. B. Leinweber, D. H. Lu, and A. W. Thomas, Phys. Rev. D **60**, 034014 (1999); Report No. ADP-99-18-T360, hep-ph/9905414.
[6] A. W. Thomas, Adv. Nucl. Phys. **13**, 1 (1984); G. A. Miller, Int. Rev. Nucl. Phys. **2**, 190 (1984).
[7] UKQCD Collaboration, C. R. Allton *et al.*, Phys. Rev. D **60**, 034507 (1999).
[8] A. W. Thomas and G. Krein, Phys. Lett. B **456**, 5 (1999).
[9] E. Jenkins, Nucl. Phys. **B368**, 190 (1992).
[10] R. F. Lebed, Nucl. Phys. **B430**, 295 (1994).
[11] M. K. Banerjee and J. Milana, Phys. Rev. D **54**, 5804 (1996).
[12] D. B. Leinweber, Nucl. Phys. **A470**, 477 (1987); R. K. Bhaduri, L. E. Cohler, and Y. Nogami, Nuovo Cimento A **65**, 376 (1981); E. Eichten, K. Gottfried, T. Kinoshita, K. D. Lane, and T. M. Yan, Phys. Rev. D **21**, 203 (1980).
[13] S. Theberge, A. W. Thomas, and G. A. Miller, Phys. Rev. D **22**, 2838 (1980); **23**, 2106(E) (1981).
[14] K. Jansen and R. Sommer, Nucl. Phys. **B530**, 185 (1998).
[15] D. H. Lu, A. W. Thomas, and A. G. Williams, Phys. Rev. C **57**, 2628 (1998).
[16] D. H. Lu, K. Tsushima, A. W. Thomas, A. G. Williams, and K. Saito, Phys. Lett. B **441**, 27 (1998); E. A. Veit *et al.*, Phys. Rev. D **31**, 1033 (1985).
[17] E. A. Veit, A. W. Thomas, and B. K. Jennings, Phys. Rev. D **31**, 2242 (1985).
[18] A. W. Thomas, J. Phys. G **7**, L283 (1981).
[19] A. Chodos, R. L. Jaffe, K. Johnson, C. B. Thorn, and V. F. Weisskopf, Phys. Rev. D **9**, 3471 (1974).
[20] A. Chodos, R. L. Jaffe, K. Johnson, and C. B. Thorn, Phys.

Rev. D **10**, 2599 (1974).
[21] T. DeGrand, R. L. Jaffe, K. Johnson, and J. Kiskis, Phys. Rev. D **12**, 2060 (1975).
[22] T. Kitagaki *et al.*, Phys. Rev. D **28**, 436 (1983).
[23] R. Bockmann, C. Hanhart, O. Krehl, S. Krewald, and J. Speth, Phys. Rev. C **60**, 055212 (1999); A.W. Thomas and K. Holinde, Phys. Rev. Lett. **63**, 2025 (1989); P.A. Guichon, G. A. Miller, and A. W. Thomas, Phys. Lett. **124B**, 109 (1983).
[24] R. Sommer, Nucl. Phys. **B411**, 839 (1994).